Is the C_2H+H_2O Reaction Anomalous?

Yi-hong Ding,* Xiang Zhang, Ze-sheng Li, Xu-ri Huang, and Chia-chung Sun

State Key Laboratory of Theoretical and Computational Chemistry, Institute of Theoretical Chemistry, Jilin University, Changchun 130023, People's Republic of China

Received: December 20, 2000; In Final Form: May 16, 2001

B3LYP/6-311G(d,p), MP2/6-311G(d,p) and CCSD(T)/6-311+G(2d,2p) (single-point) methods are employed to investigate the doublet potential-energy surface of the C_2H+H_2O radical reaction. It is shown that the quasi-direct hydrogen abstraction leading to product C_2H_2+OH is kinetically much more competitive than other dissociation or association−elimination processes. Further higher-level CCSD(T)/6-311+G(3df,2p)//QCISD/6-311G(d,p)+ZPVE calculation predicts this simple H-abstraction process to possess a classical barrier height of 3.7 kcal/mol, which is larger than those for the C_2H+H_2 and C_2H+CH_4 reactions. The calculated rate constants of the direct hydrogen abstraction process indicate that the title reaction is very slow near room temperature and may be of less importance than previously expected. Our results show that the C_2H+H_2O radical reaction is a normal quasi-direct hydrogen abstraction process in keeping with the Polanyi−Evans type correlation between the k (295 K) value and the H−X bond dissociation energy (X=OH, H, CH_3, and C_2H_5). However, our results are in sharp contradiction to the recent proposal based on the experimental measurements that the title reaction is quite fast and may have an association−elimination mechanism. This calls for future experimental investigations of this radical reaction.

1. Introduction

The ethynyl radical C_2H plays an important role in a variety of fields. It is an important intermediate in fuel-rich hydrocarbon combustion processes[1] and as a dominant chain carrier during the pyrolysis of acetylene at temperatures in excess of 1800 K.[2,3] It is also one of the most abundant species in interstellar space[4] and planetary atmosphere.[5] A number of experimental[6−30] and theoretical[29−36] investigations have been carried out on the rate constants or potential-energy surface (PES) of the C_2H reactions with a variety of neutral molecules such as H_2, CH_4, C_2H_2, C_2H_4, C_2H_6, C_3H_8, H_2O, O_2, and NO, etc.

It has been shown[23] that for H_2, CH_4, and C_2H_6, whose reaction mechanism is a direct hydrogen abstraction, there is an empirical Polanyi−Evans type correlation between the k (295 K) value and the H−X bond dissociation energy, $D_{(H-X)}$. The $D_{(H-X)}$ values are 103.3, 102.7, and 99 kcal/mol for X = H, CH_3, and C_2H_5, respectively, while the corresponding rate constants $k_{(295K)}$ are $(4-5)\cdot10^{-13}$,[18,19] $2.9\cdot10^{-12}$,[29] and $3.6\cdot10^{-11}$ cm^3 molecule^{-1} s^{-1}.[15] The most exothermic reaction is clearly the fastest. Then, the reaction of C_2H with H_2O should be much slower than the above three reactions since the $D_{(H-O)}$ value is 118 kcal/mol. However, recent experimental measurements by Van Look and Peeters[23] obtained very large rate constants for this reaction with the expression $k = (1.9 \pm 0.2)\cdot10^{-11}\exp[(-200 \pm 30)/T(\mathrm{K})]$ cm^3 molecule^{-1} s^{-1} within 295−451 K. The 295 K value is $(9.5 \pm 1.0)\cdot10^{-12}$ cm^3 molecule^{-1} s^{-1}. This indicates that the reaction of C_2H with H_2O is much faster than those with H_2 and even CH_4 and thus violates the Polanyi−Evans type correlation. Van Look and Peeters proposed that instead of a direct H-abstraction process, the title reaction might proceed to form an initial complex that would facilely isomerize to CH_2COH or HCCHOH, which may subsequently dissociate to CH_2CO+H or C_2H_2+OH. On the basis of their experimental data, Van Look and Peeters further suggested that the reaction of C_2H with H_2O could be fast enough to be a major C_2H-loss mechanism in hydrocarbon flames and would become dominant in the postcombustion region. Furthermore, we feel that if the reaction is as fast as indicated by the measured rate constants, the title reaction should also play a very important role in the depletion of C_2H radical in interstellar space.

The ab initio method has been a very powerful tool to assist in experimental determination on chemical reactions and to predict properties of reactions that are presently unknown or difficult to conduct. For the title reaction, though the rate constants within 295−451 K are known, the total reaction mechanism is still uncertain. In fact, Van Look and Peeters stated: "one must admit that there is reason to doubt that the C_2H+H_2O reaction (i) is a direct H-abstraction process and (ii) produces (only) C_2H_2 plus OH". In view of the observed surprisingly high reactivity of C_2H with H_2O and the potential importance of this reaction in both combustion and interstellar processes, we decided to carry out a detailed theoretical investigation on the potential-energy surface of C_2H_3O to ascertain its reaction mechanism. As can be seen in the text, our results indicate that the reaction is slow and of the "normal" quasi-direct H-abstraction type, in sharp contradiction to Van Look and Peeters's results.

2. Computational Methods

All structures of stationary points including minimum isomers, transition states, reactants, and products are calculated at the B3LYP/6-311G(d,p) level. For some transition states, MP2/6-311G(d,p) calculations are performed. To obtain reliable energies, single-point CCSD(T)/6-311+G(2d,2p) calculations are carried out at the B3LYP or MP2 geometries. The stationary nature of various structures is confirmed by harmonic vibration frequency calculations, i.e., isomers possess all real frequencies, whereas transition states possess one and only one imaginary frequency. The zero-point vibration energies (ZPVE) calculated at the B3LYP or MP2 level are included. To test whether the

10.1021/jp0045484 CCC: $20.00
Published on Web 08/14/2001

obtained transition states connect the right isomers, intrinsic reaction coordinate (IRC) calculations are carried out at the B3LYP or MP2 level. For the H-abstraction reaction, $C_2H+H_2O \rightarrow C_2H_2+OH$, comparative QCISD/6-311G(d,p) and CCSD(T)/6-311+G(3df,2p) (single-point) computations are carried out to obtain a more solid mechanism. All of the above calculations are performed using *Gaussian 98*.[37] Further, to give an estimate of the rate constants of the H-abstraction reaction in comparison with the experimental measurements, *POLYRATE8.0*[38] is used. The theoretical rate constants are calculated using the conventional transition state theory (TST), canonical variational transition state theory (CVT), and canonical variational transition state incorporating the small-curvature tunneling correction (CVT/SCT) method. All internal modes of the transitions states, reactants, and products are treated as harmonic vibrations.

3. Results and Discussions

For the C_2H+H_2O reaction, the potential-energy surface C_2H_3O is involved. The structures of C_2H_3O intermediate isomers are shown in Figure 1. The structures of interconversion and dissociation transition states are depicted in Figure 2. A schematic PES of C_2H_3O is plotted in Figure 3. The total and relative energies of various species are listed in Tables 1 and Table 2, respectively. In addition, the total and relative energies of the critical structures **R** C_2H+H_2O, **10** HCC...OH_2, **TS10/P1** and **P1** C_2H_2+OH at various levels are collected in Table 3, and their harmonic vibration frequencies are listed in Table 4. Finally, the calculated rate constants for the quasi-direct H-abstraction reaction at the MP2/6-311G(d,p) and QCISD/6-311G(d,p) levels are given in Table 5.

3.1. Reactant and Products. In Table 1, the total energy of the reactant **R** C_2H+H_2O is taken as zero for reference. Many dissociation products are considered here. However, only five products, i.e., **P1** (C_2H_2+OH), **P2** (CH_2CO+H), **P3** (HCCOH+H), **P5** (CH_3+CO), and **P6** ($HCCO+H_2$), may be thermodynamically possible, and these lie at −14.6, −35.0, −0.6, −78.8, and −30.9 kcal/mol, respectively at the CCSD(T)/6-311+G(2d,2p)/B3LYP/6-311G(d,p) +ZPVE level. For simplicity, the energies are all at this level unless specified in the following discussions. The remaining products lie much higher (more than 24 kcal/mol) above reactant **R** and will not be considered in later discussions.

3.2. Intermediate Isomers. Ten C_2H_3O isomers are obtained as minima. The lowest energy isomer is **1,** CH_3CO, at −77.5 kcal/mol. The second and third lowest-lying species **2,** CH_2-CHO (I) (−70.1 kcal/mol), and **3**, CH_2CHO (II) (−47.5 kcal/mol), are a pair of resonant isomers with two valence structures. Isomer **2** in $^2A''$ state with a C═O double bond is about 22.6 kcal/mol lower than isomer **3** in $^2A'$ state with a C−O single bond. The energy difference between **2** and **3** is in excellent agreement with the experimental value 0.99 eV (i.e., 22.83 kcal/mol).[39] Isomer **2** can be viewed as an addition product between HCO and CH_2 radicals, whereas isomer **3** can be formed between the C_2H_3 and O radicals. It should be pointed out that a number of experimental and theoretical investigations have been published on the three isomers concerning their structures and dissociation mechanisms (see Osborn et al.[40] and references cited herein).

Isomer **4,** CH_2COH, can be seen as formed between the H_2C═C and OH radicals. It is also very low-lying at −46.0 kcal/mol and lies just 1.5 kcal/mol above isomer **2**. The isomers **5**−**8** are four cis and trans forms labeled by HCCHOH (I), (II), (III), and (IV), respectively. All can be formed via the direct addition of OH radical at one carbon site of the acetylene C_2H_2,

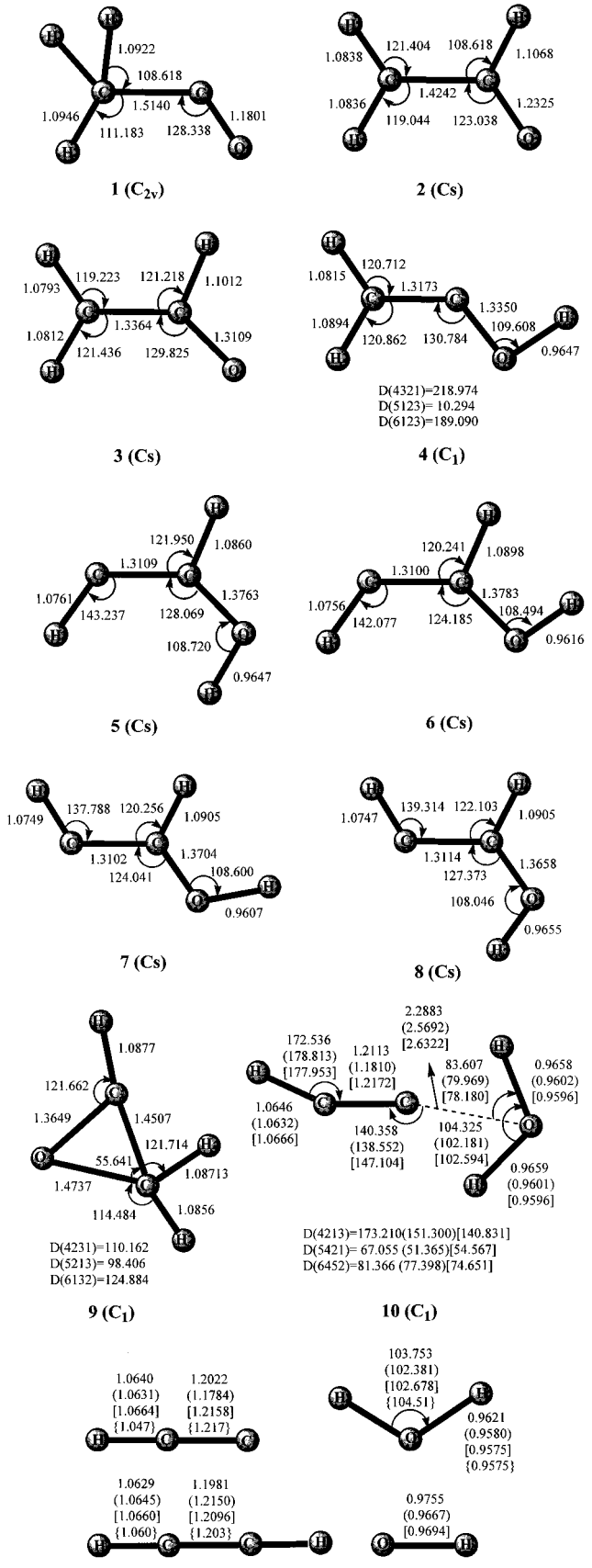

Figure 1. Optimized structures of C_2H_3O isomers at the B3LYP/6-311G(d,p). The structures of the fragments C_2H, H_2O, C_2H_2 and OH are also given. The values in parentheses, square brackets, and curly brackets, {}, are at the MP2/6-311G(d,p), QCISD/6-311G(d,p), and experimental level, respectively (C_2H structure from Bogey et al.[41] and C_2H_2 and H_2O structures from Lide[42]). Bond lengths are in angstroms and angles are in degrees.

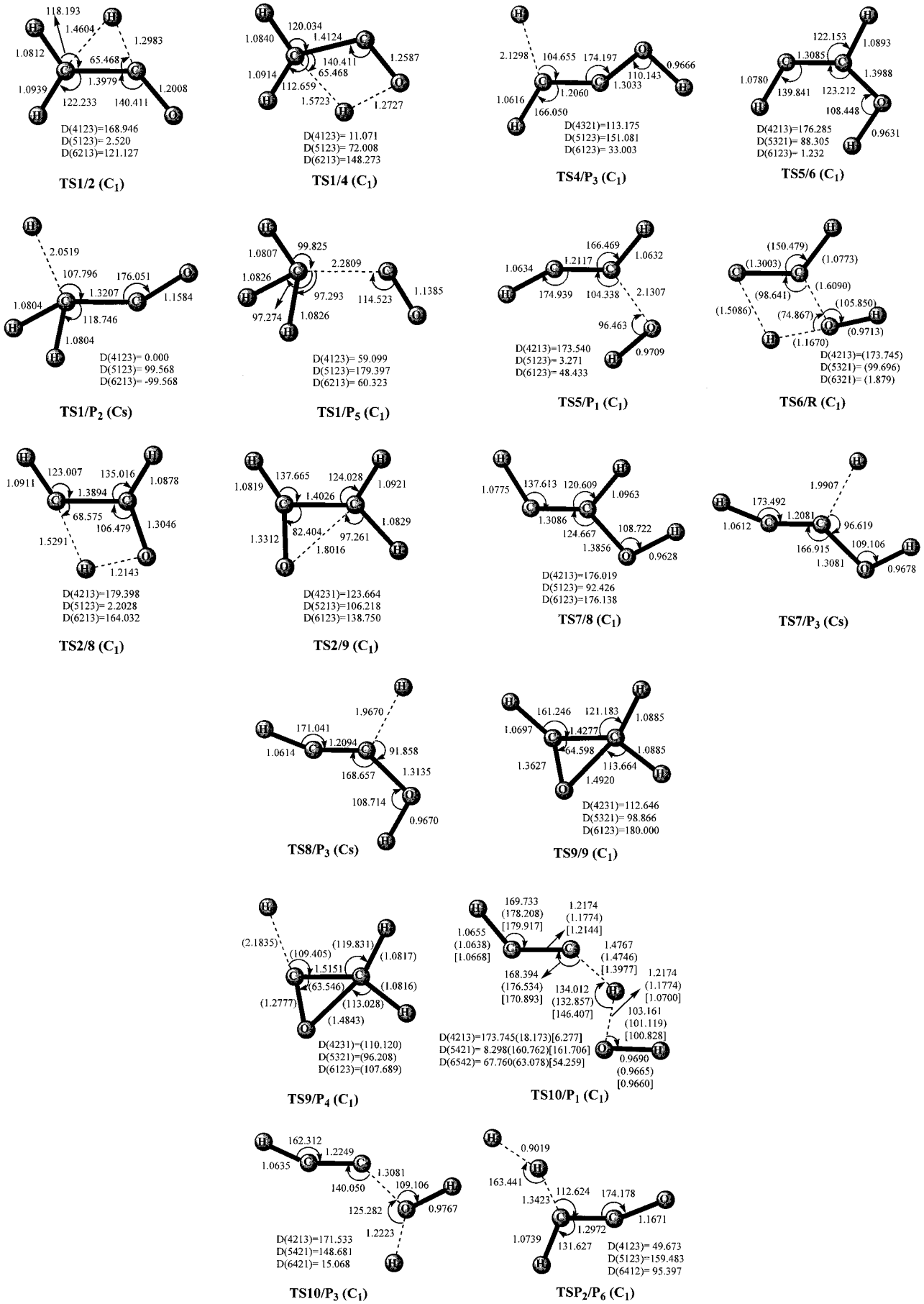

Figure 2. Optimized structures of C_2H_3O transition states at the B3LYP/6-311G(d,p), MP2/6-311G(d,p) (in parentheses), or QCISD/6-311G(d,p) (in square brackets) levels. Bond lengths are in angstroms and angles are in degrees.

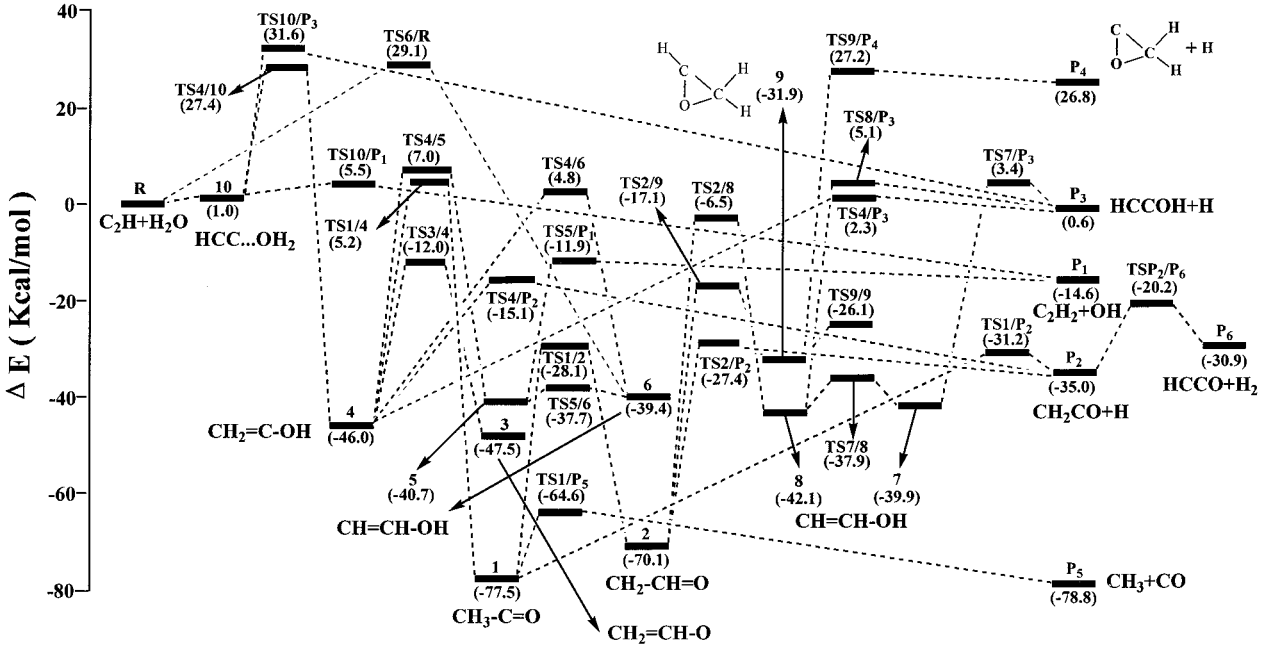

Figure 3. Schematic potential-energy surface of C_2H_3O at the CCSD(T)/6-311+G(2d,2p) level.

TABLE 1: Total[a] and Relative[b] Energies of the C_2H_3O Reactant, Products, and Isomers at the B3LYP/6-311G(d,p) and Single-Point CCSD(T)/6-311+G(2d,2p)//B3LYP/6-311G(d,p) Levels

	species	B3LYP/6-311G(d,p)	CCSD(T)/6-311+G(2d,2p)	CCSD(T)/6-311+G(2d,2p)+ZPVE
R	C_2H+H_2O	−153.076 906 4 (0.0)	−152.749 855 9 (0.0)	(0.0)
P1	C_2H_2+OH	−153.109 225 2 (−20.3)	−152.773 071 0 (−14.6)	(−14.6)
P2	CH_2CO+H	−153.149 908 6 (−45.8)	−152.801 861 0 (−32.6)	(−35.0)
P3	HCCOH+H	−153.089 637 5 (−8.0)	−152.747 136 2 (1.7)	(−0.6)
P4	$cOCCH_2+H$	−153.043 845 8 (20.7)	−152.703 832 1 (28.9)	(26.8)
P5	CH_3+CO	−153.199 992 9 (−77.2)	−152.864 601 3 (−72.0)	(−78.8)
P6	$HCCO+H_2$	−153.148 470 9 (−44.9)	−152.793 031 4 (−27.1)	(−30.9)
P7	$^1CH_2+HCO$	−153.030 952 9 (28.8)	−152.693 378 2 (35.4)	(31.6)
P8	$^3CH_2+HCO$	−153.051 066 3 (16.2)	−152.710 971 2 (24.4)	(21.0)
P9	$^1CH_2+HOC$	−152.963 966 8 (70.9)	−152.628 312 4 (76.3)	(72.7)
P10	$^3CH_2+HOC$	−152.984 080 2 (58.2)	−152.645 905 4 (65.2)	(62.0)
P11	$C_2H_3+^1O$	−152.910 280 7 (104.6)	−152.592 124 4 (99.0)	(99.6)
P12	$C_2H_3+^3O$	−153.012 406 9 (40.5)	−152.675 706 0 (46.5)	(47.1)
1	CH_3CO	−153.226 767 7 (−94.0)	−152.880 855 5 (−82.2)	(−77.5)
2	CH_2CHO (I)	−153.216 862 1 (−87.8)	−152.868 410 7 (−74.4)	(−70.1)
3	CH_2CHO (II)	−153.182 953 5 (−66.5)	−152.832 739 4 (−52.0)	(−47.5)
4	CH_2COH	−153.176 990 2 (−62.8)	−152.830 476 9 (−50.6)	(−46.0)
5	HCCHOH (I)	−153.166 890 7 (−56.5)	−152.821 863 4 (−45.2)	(−40.7)
6	HCCHOH (II)	−153.163 191 2 (−54.1)	−152.819 308 9 (−43.6)	(−39.4)
7	HCCHOH (III)	−153.163 575 8 (−54.4)	−152.820 203 6 (−44.1)	(−39.9)
8	HCCHOH (IV)	−153.169 023 1 (−57.8)	−152.824 049 3 (−46.6)	(−42.1)
9	$H\text{-}cCOCH_2$	−153.156 382 1 (−49.9)	−152.809 052 5 (−37.1)	(−31.9)
10	$HCC...OH_2$	−153.091 475 4 (−9.1)	−152.752 129 4 (−1.4)	(1.0)

[a] In atomic units. [b] In kilocalorie per mole. Shown in parentheses.

The four isomers are energetically low-lying with the corresponding relative energies being −40.7, −39.4, −39.9, and −42.1 kcal/mol. Isomer **9** possesses a CCO three-membered ring structure with two H located on one C and one H on the other C. It lies higher than the former chainlike species, yet still at −31.9 kcal/mol. Isomer **10** is in fact a weakly bound structure between the C_2H radical and the polar H_2O molecule. At the CCSD(T)/6-311+G(2d,2p) single-point level without ZPVE correction, it lies just 1.4 kcal/mol below the reactant **R**. However, inclusion of ZPVE lays it even 1.0 kcal/mol above **R**. In fact, further higher-level CCSD(T)/6-311+G(3df,2p)//QCISD/6-311G(d,p) calculation, as can be seen in Table 3, confirms the existence of the weakly bound complex **10**, although it is just 0.6 kcal/mol below **R** with ZPVE correction. This indicates that isomer **10** is truly a stationary structure and is quite unstable toward decomposition even at 0 K.

3.3. Potential-Energy Surface Feature of C2H3O. To obtain a detailed mechanism of the C_2H+H_2O reaction, we search for various isomerization or as many as possible dissociation transition states to connect the 10 isomers. Figure 3 represents a schematic PES of C_2H_3O. By means of the depth of the potential well that the isomers reside in, we can then discuss their kinetic stability.

The kinetic stability of the lowest-lying isomer, **1** (CH_3CO), is governed by its dissociation to CH_3 and CO via **TS1/P5** with the dissociation barrier of 12.9 kcal/mol. Its H-elimination to **P2** (CH_2CO+H) needs 46.3 kcal/mol, whereas its isomerization to isomer **2** (CH_2–Ch═O) via 1,2 H-shift and to isomer **4** (CH_2-

TABLE 2: Total[a] (a.u.) and Relative[b] Energies of the C_2H_3O Transition States at the B3LYP/6-311G(d,p) and Single-Point CCSD(T)/6-311+G(2d,2p)// //B3LYP/6-311G(d,p) Levels

species	B3LYP/6-311G(d,p)	CCSD(T)/6-311+G(2d,2p)	CCSD(T)/6-311+G(2d,2p)+ZPVE
TS1/2	−153.150 590 2 (−46.2)	−152.797 421 8 (−29.8)	(−28.1)
TS1/4	−153.091 752 5 (−9.3)	−152.741 654 6 (5.1)	(5.2)
TS1/P2	−153.150 575 8 (−46.2)	−152.797 459 0 (−29.9)	(−31.2)
TS1/P5	−153.196 237 7 (−74.9)	−152.855 181 2 (−66.1)	(−64.6)
TS2/8	−153.113 240 9 (−22.8)	−152.761 938 0 (−7.6)	(−6.5)
TS2/9	−153.131 527 5 (−34.3)	−152.782 561 8 (−20.5)	(−17.1)
TS2/P2	−153.143 547 4 (−41.8)	−152.791 592 5 (−26.2)	(−27.4)
TS3/4	−153.119 735 0 (−26.9)	−152.767 901 7 (−11.3)	(−12.0)
TS4/5	−153.087 978 2 (−6.9)	−152.739 204 3 (6.7)	(7.0)
TS4/6	−153.091 355 4 (−9.1)	−152.743 447 2 (4.0)	(4.8)
TS4/10	−153.052 459 8 (15.3)	−152.706 442 7 (27.2)	(27.4)
TS4/P2	−153.130 063 4 (−33.4)	−152.771 335 2 (−13.5)	(−15.1)
TS4/P3	−153.089 448 6 (−7.9)	−152.742 859 3 (4.4)	(2.7)
TS5/6	−153.158 514 1 (−51.2)	−152.815 916 2 (−41.5)	(−37.7)
TS5/P1	−153.113 955 3 (−23.2)	−152.770 813 8 (−13.2)	(−11.9)
TS6/R[c]		−152.706 630 2 (27.1)	(29.1)
TS7/8	−153.158 512 9 (−51.2)	−152.816 033 9 (−41.5)	(−37.9)
TS7/P3	−153.088 772 6 (−7.4)	−152.742 385 3 (4.7)	(3.4)
TS8/P3	−153.085 584 4 (−5.4)	−152.739 534 0 (6.5)	(5.1)
TS9/9	−153.146 375 6 (−43.6)	−152.798 146 6 (−30.3)	(−26.1)
TS9/P4[c]		−152.704 682 4 (28.3)	(27.2)
TS10/P1	−153.085 659 6 (−5.5)	−152.740 329 2 (6.0)	(5.5)
TS10/P3	−153.049 134 2 (17.4)	−152.697 134 6 (33.1)	(31.6)
TSP2/P6	−153.135 251 9 (−36.6)	−152.776 224 3 (−16.5)	(−20.2)

[a] In atomic units. [b] In kilocalorie per mole. Shown in parentheses [c] For **TS6/R** and **TS9/P4**, the MP2/6-311G(d,p) geometries are used for single-point calculations.

TABLE 3: Total,[a] Zero-point Vibration,[a] and Relative[b] Energies of R, 10, TS10/P1, and P1 at Various Levels

levels	**R**, C_2H+H_2O	**10**, HCC...OH_2	**TS10/P1**	**P1**, C_2H_2+OH
B3LYP/6-311G(d,p)	−153.076 9064 (0.0)	−153.091 475 4 (−9.1)	−153.085 659 6 (−5.5)	−153.109 225 2 (−20.3)
CCSD(T)/6-311+G(2d,2p)// B3LYP/6-311G(d,p)	−152.749 8559 (0.0)	−152.752 129 4 (−1.4)	−152.740 329 2 (6.0)	−152.773 071 0 (−14.6)
CCSD(T)/6-311+G(3df,2p)// B3LYP/6-311G(d,p)	−152.797 6785 (0.0)	−152.800 381 7 (−1.7)	−152.789 045 0 (5.4)	−152.821 757 5 (−15.1)
ZPVE/B3LYP/6-311G(d,p)	0.035 442 (0.0)	0.039 207 (2.4)	0.034 632 (−0.5)	0.035 417 (0.0)
MP2/6-311G(d,p)	−152.642 7800 (0.0)	−152.649 059 0 (−3.9)	−152.636 149 5 (4.2)	−152.684 142 6 (−26.0)
CCSD(T)/6-311+G(2d,2p)// MP2/6-311G(d,p)	−152.747 7900 (0.0)	−152.750 774 6 (−1.9)	−152.737 554 5 (6.4)	−152.773 303 0 (−16.0)
CCSD(T)/6-311+G(3df,2p)// MP2/6-311G(d,p)	−152.795 6581 (0.0)	−152.798 889 6 (−2.0)	−152.786 478 6 (5.8)	−152.821 926 3 (−16.5)
ZPVE/MP2/6-311G(d,p)	0.039 422 (0.0)	0.041 606 (1.4)	0.038 342 (−0.7)	0.035 299 (−2.6)
QCISD/6-311G(d,p)	−152.685 737 7 (0.0)	−152.691 188 7 (−3.4)	−152.676 538 3 (5.8)	−152.713 4831 (−17.4)
CCSD(T)/6-311+G(3df,2p)// QCISD/6-311G(d,p)	−152.797 713 4 (0.0)	−152.800 927 0 (−2.0)	−152.788 558 9 (5.7)	−152.822 0029 (−15.2)
ZPVE/QCISD/6-311G(d,p)	0.0365 84 (0.0)	0.0388 91 (1.4)	0.033 466 (−2.0)	0.035 289 (−0.8)

[a] In atomic units. [b] In kilocalorie per mole. Shown in parentheses.

COH) via 1,3 H-shift needs high barriers of 49.4 and 82.7 kcal/mol, respectively. Isomer **2** (CH_2–Ch═O) lies in a much deeper potential well stabilized by the barrier of 42.0 kcal/mol for **2**→**1** conversion and 42.7 kcal/mol for the dissociation of **2** to **P2** (CH_2CO+H) via **TS2/P2**. Isomerization of **2** to the isomers **8**, HCCHOH (IV), and **9** (H−cCOCH_2) need to overcome even higher barriers (63.6 and 53.0 kcal/mol). Only one transition state, **TS3/4**, associated with the valence isomer **3** (CH_2═CH−O) is obtained. Then, **3** is separated by a considerable barrier 35.5 kcal/mol from conversion to the isomer **4** (CH_2COH), which has comparable relative energy to **3**. It should be noted that in a recent theoretical investigation by Osborn et al.,[40] the dissociation transition state of **2** to **P2** (CH_2CO+H) was not located. Instead, they found a transition state **TS3/P2** (in C_1 symmetry) connecting **3** and **P2**, which cannot be obtained at both B3LYP and MP2 levels in this paper. Any optimization of **TS3/P2** would inevitably lead to **TS2/P2**, which is confirmed by IRC calculations. Interestingly, as shown in Figure 1, the CC bond length (1.3313 Å) of **TS2/P2** is almost the same as that (1.3364 Å) of isomer **3**, while its CO bond length (1.1630 Å) is closer to that (1.2325 Å) of isomer **2** than to that (1.3109 Å) of isomer **1**. Also, we preliminarily hope to find a transition state linking **3** and the isomer **8,** HCCHOH (IV). However, it often leads to **TS2/8, as** confirmed by IRC calculations. As can be seen from Table 2, the direct dissociation of **2** to **P8** ($^3CH_2$+HCO) and **3** to **P12** (C_2H_3+^{3}O) is almost impossible due to the large barriers of 91.1 and 94.6 kcal/mol, respectively.

The isomer **4** CH_2COH has seven conversion channels. Via 1,2 or 1,3 H-migrations, **4** can isomerize to **1** (CH_3CO), **3** (CH_2-CHO (II)), **5** (HCCHOH (I)), **6** (HCCHOH (II)), and **10** (HCC...OH_2) with the barriers of 51.2, 34.0, 53.0, 50.8, and 73.4 kcal/mol, respectively. It can also take direct H-elimination processes to **P2** (CH_2CO+H) and **P3** (HCCOH+H) with the corresponding barriers of 30.9 and 33.3 kcal/mol. Surely, the **4**→**3** conversion with the barrier of 34.0 kcal/mol governs the kinetic stability of isomer **4**.

There exist very small barriers for interconversion between the cis−trans isomers HCCHOH **5** and **6** and between **7** and **8**. The barriers are 3.0, 1.7, 2.0, and 4.2 kcal/mol for **5**→**6**, **6**→**5**, **7**→**8,** and **8**→**7** conversions, respectively. This is understandable since the OH bond just rotates along the C−O single bond. On the other hand, we are not able to locate the transition state between **5** and **8**, **6** and **7**, **5** and **7**, and **6** and **8**. We suggest that even though these transition states exist, larger barriers are needed due to the hindrance of rotation along C═C double bond. Despite the easiness of interconversion between **5** and **6** and between **7** and **8**, isomerization to other isomers or dissociation to fragments is quite difficult. The conversion barriers for **5**→**4**,

TABLE 4: Harmonic Vibration Frequencies (cm^{-1}) and Infrared Intensities (kml/mol) of the Critical Species C_2H, H_2O, 10, TS10/P1, C_2H_2, and OH at Various Levels and $\langle S^2 \rangle$ Values at B3LYP and MP2 Levels

species	$\langle S^2 \rangle$	levels	harmonic vibration frequencies (infrared intensities)
C_2H	0.77	B3LYP	328 (4) 329 (3) 2089 (6) 3463 (55)
	1.05	MP2	838 (16) 838 (16) 2471 (9) 3577 (59)
		QCISD	473 (6) 473 (6) 2043 (4) 3486 (52)
		expt.[a]	372 372 1840 3298
H_2O		B3LYP	1639 (58) 3808 (4) 3905 (25)
		MP2	1669 (51) 3902 (6) 4010 (33)
		QCISD	1689 (51) 3900 (4) 3994 (23)
		expt.[b]	1595 3657 3756
10	0.77	B3LYP	30 (34) 78 (4) 271 (68) 427 (10) 451 (250) 612 (49) 618 (34) 1618 (64) 2014 (34) 3449 (50) 3772 (52) 3869 (77)
	1.04	MP2	93 (13) 97 (50) 119 (55) 327 (9) 357 (352) 839 (31) 855 (23) 1665 (55) 2471 (3) 3575 (67) 3880 (20) 3985 (53)
		QCISD	62 (1) 88 (39) 116 (44) 311 (12) 333 (328) 553 (32) 560 (19) 1684 (57) 2036 (3) 3483 (52) 3876 (26) 3970 (38)
TS10/P1	0.76	B3LYP	747*i* (33) 97 (12) 150 (44) 357 (44) 602 (62) 626 (81) 685 (63) 1400 (62) 1925 (58) 2137 (295) 3439 (18) 3785 (94)
	1.01	MP2	1082*i* (405) 107 (10) 143 (35) 336 (49) 600 (137) 874 (27) 892 (29) 1464 (29) 2304 (826) 2661 (67) 3591 (97) 3856 (96)
		QCISD	1638*i* (1276) 110 (11) 130 (1) 356 (27) 565 (114) 628 (58) 652 (38) 1169 (101) 1642 (438) 2106 (8) 3483 (63) 3848 (67)
C_2H_2		B3LYP	643 (0) 773 (96) 2070 (0) 3420 (88) 3523 (0)
		MP2	561 (0) 769 (89) 1970 (0) 3461 (92) 3551 (0)
		QCISD	577 (0) 774 (88) 2024 (0) 3438 (80) 3536 (0)
		expt.[b]	612 730 1974 3289 3374
OH	0.75	B3LYP	3701 (6)
	0.75	MP2	3852 (11)
		QCISD	3790 (4)

[a] From Temsaman and Hennan.[43] [b] From Lide.[42]

TABLE 5: Rate Constants (cm^3 $molecule^{-1}$ s^{-1}) for the C_2H+H_2O Reaction within the Temperature Range 20−4500 K

T (K)	TST[a]	CVT[a]	CVT/SCT[a]	TST[b]	CVT/SCT[c]	expt.[d]	CVT/SCT[e]
20	$1.61 \cdot 10^{-49}$	$1.44 \cdot 10^{-49}$	$5.59 \cdot 10^{-15}$	$2.44 \cdot 10^{-66}$			*$5.88 \cdot 10^{-15}$*
30	$4.27 \cdot 10^{-37}$	$3.95 \cdot 10^{-37}$	$3.31 \cdot 10^{-15}$	$2.61 \cdot 10^{-48}$			*$4.41 \cdot 10^{-15}$*
40	$6.22 \cdot 10^{-31}$	$5.88 \cdot 10^{-31}$	$2.36 \cdot 10^{-15}$	$2.42 \cdot 10^{-39}$			*$3.81 \cdot 10^{-15}$*
50	$2.95 \cdot 10^{-27}$	$2.82 \cdot 10^{-27}$	$1.89 \cdot 10^{-15}$	$5.51 \cdot 10^{-34}$			*$3.65 \cdot 10^{-15}$*
60	$8.11 \cdot 10^{-25}$	$7.84 \cdot 10^{-25}$	$1.64 \cdot 10^{-15}$	$6.01 \cdot 10^{-30}$			*$3.79 \cdot 10^{-15}$*
80	$8.87 \cdot 10^{-22}$	$8.68 \cdot 10^{-22}$	$1.44 \cdot 10^{-15}$	$5.53 \cdot 10^{-26}$			*$4.96 \cdot 10^{-15}$*
100	$5.87 \cdot 10^{-20}$	$5.79 \cdot 10^{-20}$	$1.46 \cdot 10^{-15}$	$2.54 \cdot 10^{-23}$	$6.32 \cdot 10^{-18}$		*$7.81 \cdot 10^{-15}$*
120	$9.68 \cdot 10^{-19}$	$9.6 \cdot 10^{-19}$	$1.62 \cdot 10^{-15}$	$1.52 \cdot 10^{-21}$	$2.54 \cdot 10^{-18}$		*$1.35 \cdot 10^{-14}$*
150	$1.63 \cdot 10^{-17}$	$1.62 \cdot 10^{-17}$	$2.18 \cdot 10^{-15}$	$9.33 \cdot 10^{-20}$	$1.25 \cdot 10^{-17}$		*$3.12 \cdot 10^{-14}$*
178	$9.88 \cdot 10^{-17}$	$9.86 \cdot 10^{-17}$	$3.18 \cdot 10^{-15}$	$1.27 \cdot 10^{-18}$	$4.07 \cdot 10^{-17}$		*$6.31 \cdot 10^{-14}$*
180	$1.10 \cdot 10^{-16}$	$1.10 \cdot 10^{-16}$	$3.27 \cdot 10^{-15}$	$1.49 \cdot 10^{-18}$	$4.43 \cdot 10^{-17}$		*$6.60 \cdot 10^{-14}$*
191	$1.92 \cdot 10^{-16}$	$1.92 \cdot 10^{-16}$	$3.85 \cdot 10^{-15}$	$3.33 \cdot 10^{-18}$	$6.68 \cdot 10^{-17}$		*$8.44 \cdot 10^{-14}$*
213	$4.98 \cdot 10^{-16}$	$4.97 \cdot 10^{-16}$	$5.38 \cdot 10^{-15}$	$1.31 \cdot 10^{-17}$	$1.41 \cdot 10^{-16}$		*$1.32 \cdot 10^{-13}$*
215	$5.38 \cdot 10^{-16}$	$5.38 \cdot 10^{-16}$	$5.55 \cdot 10^{-15}$	$1.47 \cdot 10^{-17}$	$1.52 \cdot 10^{-16}$		*$1.37 \cdot 10^{-13}$*
228	$8.64 \cdot 10^{-16}$	$8.63 \cdot 10^{-16}$	$6.77 \cdot 10^{-15}$	$2.89 \cdot 10^{-17}$	$2.27 \cdot 10^{-16}$		*$1.73 \cdot 10^{-13}$*
293	$5.17 \cdot 10^{-15}$	$5.17 \cdot 10^{-15}$	$1.73 \cdot 10^{-14}$	$3.67 \cdot 10^{-16}$	$1.23 \cdot 10^{-15}$		*$4.54 \cdot 10^{-13}$*
295	$5.40 \cdot 10^{-15}$	$5.40 \cdot 10^{-15}$	$1.77 \cdot 10^{-14}$	$3.91 \cdot 10^{-16}$	$1.28 \cdot 10^{-15}$	$9.50 \cdot 10^{-12}$	*$4.60 \cdot 10^{-13}$*
298	$5.76 \cdot 10^{-15}$	$5.76 \cdot 10^{-15}$	$1.85 \cdot 10^{-14}$	$4.28 \cdot 10^{-16}$	$1.37 \cdot 10^{-15}$	$9.70 \cdot 10^{-12}$	*$4.76 \cdot 10^{-13}$*
332	$1.12 \cdot 10^{-14}$	$1.12 \cdot 10^{-14}$	$2.82 \cdot 10^{-14}$	$1.09 \cdot 10^{-15}$	$2.74 \cdot 10^{-15}$	$1.09 \cdot 10^{-11}$	
351	$1.55 \cdot 10^{-14}$	$1.55 \cdot 10^{-14}$	$3.52 \cdot 10^{-14}$	$1.70 \cdot 10^{-15}$	$3.86 \cdot 10^{-15}$	$1.06 \cdot 10^{-11}$	
385	$2.58 \cdot 10^{-14}$	$2.58 \cdot 10^{-14}$	$5.07 \cdot 10^{-14}$	$3.45 \cdot 10^{-15}$	$6.88 \cdot 10^{-15}$	$1.09 \cdot 10^{-11}$	
431	$4.63 \cdot 10^{-14}$	$4.62 \cdot 10^{-14}$	$7.88 \cdot 10^{-14}$	$7.67 \cdot 10^{-15}$	$1.31 \cdot 10^{-14}$	$1.19 \cdot 10^{-11}$	
451	$5.80 \cdot 10^{-14}$	$5.78 \cdot 10^{-14}$	$9.39 \cdot 10^{-14}$	$1.04 \cdot 10^{-14}$	$1.68 \cdot 10^{-14}$	$1.26 \cdot 10^{-11}$	
500	$9.46 \cdot 10^{-14}$	$9.43 \cdot 10^{-14}$	$1.39 \cdot 10^{-13}$	$2.01 \cdot 10^{-14}$	$2.95 \cdot 10^{-14}$		*$2.43 \cdot 10^{-12}$*
660	$3.15 \cdot 10^{-13}$	$3.13 \cdot 10^{-13}$	$3.89 \cdot 10^{-13}$	$9.74 \cdot 10^{-14}$	$1.20 \cdot 10^{-13}$		*$4.78 \cdot 10^{-12}$*
1000	$1.53 \cdot 10^{-12}$	$1.52 \cdot 10^{-12}$	$1.65 \cdot 10^{-12}$	$7.06 \cdot 10^{-13}$	$7.62 \cdot 10^{-13}$		*$1.11 \cdot 10^{-11}$*
1500	$6.19 \cdot 10^{-12}$	$6.19 \cdot 10^{-12}$	$6.22 \cdot 10^{-12}$	$3.69 \cdot 10^{-12}$			*$2.33 \cdot 10^{-11}$*
2000	$1.58 \cdot 10^{-11}$	$1.55 \cdot 10^{-11}$	$1.50 \cdot 10^{-11}$	$1.07 \cdot 10^{-11}$			*$4.01 \cdot 10^{-11}$*
2200	$2.13 \cdot 10^{-11}$	$2.09 \cdot 10^{-11}$	$2.01 \cdot 10^{-11}$	$1.50 \cdot 10^{-11}$			*$4.79 \cdot 10^{-11}$*
2500	$3.17 \cdot 10^{-11}$	$3.09 \cdot 10^{-11}$	$2.94 \cdot 10^{-11}$	$2.33 \cdot 10^{-11}$			*$6.32 \cdot 10^{-11}$*
2580	$3.50 \cdot 10^{-11}$	$3.40 \cdot 10^{-11}$	$3.23 \cdot 10^{-11}$	$2.59 \cdot 10^{-11}$			*$6.87 \cdot 10^{-11}$*
2800	$4.49 \cdot 10^{-11}$	$4.34 \cdot 10^{-11}$	$4.12 \cdot 10^{-11}$	$3.41 \cdot 10^{-11}$			*$8.10 \cdot 10^{-11}$*
3000	$5.54 \cdot 10^{-11}$	$5.33 \cdot 10^{-11}$	$5.05 \cdot 10^{-11}$	$4.28 \cdot 10^{-11}$			*$9.43 \cdot 10^{-11}$*
3200	$6.73 \cdot 10^{-11}$	$6.45 \cdot 10^{-11}$	$6.11 \cdot 10^{-11}$	$5.28 \cdot 10^{-11}$			*$1.09 \cdot 10^{-10}$*
3500	$8.79 \cdot 10^{-11}$	$8.38 \cdot 10^{-11}$	$7.94 \cdot 10^{-11}$	$7.04 \cdot 10^{-11}$			*$1.32 \cdot 10^{-10}$*
3800	$1.12 \cdot 10^{-10}$	$1.06 \cdot 10^{-11}$	$1.01 \cdot 10^{-10}$	$9.14 \cdot 10^{-11}$			*$1.59 \cdot 10^{-10}$*
4000	$1.30 \cdot 10^{-10}$	$1.23 \cdot 10^{-10}$	$1.17 \cdot 10^{-10}$	$1.07 \cdot 10^{-10}$			*$1.78 \cdot 10^{-10}$*
4500	$1.83 \cdot 10^{-10}$	$1.73 \cdot 10^{-10}$	$1.64 \cdot 10^{-10}$	$1.54 \cdot 10^{-10}$			*$2.30 \cdot 10^{-10}$*

[a] At the MP2/6-311G(d,p) level. [b] At the CCSD(T)/6-311+G(3df,2p)//QCISD/6-311G(d,p) level. [c] The CCSD(T)/6-311+G(3df,2p)//QCISD/6-311G(d,p) k(TST) values multiplied by the scaling factors $k_{(CVT/SCT)}/k_{(TST)}$ obtained at the MP2/6-311G(d,p) level. [d] Experimental values for the C_2H+H_2O reaction from Van Look and Peeters.[23] [e] The italic values are theoretical for the C_2H+H_2 reaction from Zhang et al.[36]

5→P1, **6→4**, **6→R**, **7→P3**, **8→2,** and **8→P3** are very large: 47.7, 38.8, 44.2, 69.5, 43.3, 35.6, and 47.2, respectively.

The cyclic isomer **9** (H-c$COCH_2$) is stabilized by at least 14.8 kcal/mol for **9→2** conversion. Its direct dissociation to **P4** (c$OCCH_2$+H) needs 59.1 kcal/mol. **TS9/9** is associated with the automerization of **9**. The weakly bound isomer **10** can dissociate to **R** (C_2H+H_2O) with no barrier. The dissociation of **10** to **P1** (C_2H_2+OH) and **P3** (HCCOH+H) needs 4.5 and

30.6 kcal/mol, respectively, whereas isomerization to **4** (CH_2-COH) needs 26.4 kcal/mol.

From the above discussions, we can see that the isomers **2**−**8** have considerable kinetic stability of more than 30 kcal/mol (the easy interconversion between **5** and **6**, and **7** and **8** indicates that all four isomers may coexist). The lowest-lying isomer, **1**, has relatively much lower kinetic stability. It should be pointed out that although the relative energy of **P6** ($HCCO+H_2$) is very low (−30.9 kcal/mol), we are not able to locate any H_2-elimination transition states of the isomers **1**, **2**, **6** and **7** despite many attempts. Since such processes may involve complex bond rearrangement, higher barriers are expected to exist for these than for the single H-elimination process. Thus, absence of these H_2-elimination transition states may not affect the kinetic stability of the C_2H_3O isomers. As a secondary reaction, we locate **TSP2/P6** that is associated with the H-abstraction between CH_2CO and H in **P2** to give $HCCO+H_2$ in **P6**.

3.4. Reaction Mechanism. On the basis of the PES of C_2H_3O as shown in Figure 3, let us discuss the mechanism of the C_2H+H_2O radical reaction. As discussed in section 3.1, five products, **P1** (C_2H_2+OH; −14.6), **P2** (CH_2CO+H; −35.0), **P3** (HCCOH+H; −0.6), **P5** (CH_3+CO; −78.8), and **P6** ($HCCO+H_2$; −30.9), are energetically allowed. However from Figure 3, we can see that starting from the reactant **R**, there are no barrierless reaction pathways to form the five products.

Two kinds of reaction channels exist for this reaction, namely "quasi-direct" and "indirect" channels. The quasi-direct channel includes the following two pathways. Path 1: **R** (0.0)→**10** (1.0)→**TS10/P1** (5.5)→**P1** (−14.6). Path 2: **R** (0.0)→**10** (1.0)→**TS10/P3** (31.6)→**P3** (−0.6). The values in parentheses are single-point CCSD(T)/6-311+G(2d,2p) relative energies taken from Table 2. Except the very unstable complex **10**, no intermediate is involved. Path 1 is associated with a hydrogen atom transfer from H_2O to the C_2H radical. Then, Path 1 is also named a "quasi-direct H-abstraction process". Path 2 is a quasi-direct concerted association−elimination process.

The indirect channel involves complicated pathways that may lead to various products. Yet, the initial steps are the following two pathways. Path 3: **R** (0.0)→**10** (1.0)→**TS4/10** (27.4)→**4** (−46.0). Path 4: **R** (0.0)→**TS6/R** (29.1)→**6** (−39.4). Subsequent isomerization or dissociation may then form the five products. Both pathways involve at least one low-lying or kinetically stable intermediate. So they are also generally called "association−elimination processes".

Simply from the relative energies of the rate-determining transition states **TS10/P1** (5.5), **TS10/P3** (31.6), **TS4/10** (27.4), and **TS6/R** (29.1) within Paths 1, 2, 3**,** and 4, respectively, we can know that the most competitive reaction pathway is Path 1. So, the mechanism of the title C_2H+H_2O radical reaction is a simple quasi-direct H-abstraction process that forms the product C_2H_2 and OH. Other processes are much less probable although the involved intermediates and products are very low-lying.

It should be noted that we preliminarily hope to find an addition isomer $HCCOH_2$ that can successively isomerize to HCCHOH (**5**, **6**, **7,** or **8**) and then dissociate to **P1.** Yet optimization of $HCCOH_2$ often leads to the fragment **P3**. Also, the attempt to search for a concerted transition state that leads the reactant **R** to form the isomer HCCHOH (**5**, **6**, **7,** or **8**) fails. Instead, it often leads to **TS10/P1** with a long O−C distance. This is possibly due to the strong repulsion of the lone electron pair on the O.

3.5. Rate Constants. For the simple quasi-direct H-abstraction $C_2H+H_2O→C_2H_2+OH$ reaction, further comparative calculations are carried out for the critical structures **R**, **10**, **TS10/P1,** and **P1** at the MP2/6-311G(d,p), QCISD/6-311G(d,p) and CCSD(T)/6-311+G(3df,2p) (single-point) levels so as to obtain the dynamic properties and rate constants of this process. As shown in Figure 1, the computed 6-311G(d,p) B3LYP, MP2 and QCISD structures of C_2H, H_2O, and C_2H_2 are in close agreement with the corresponding experimental values[41,42] except that the CC bond length, 1.1784 Å, of C_2H at the MP2 level is considerably shorter than the experimental value, 1.217 Å.[41] This may partly result from the relatively high spin contamination of the C_2H radical as shown in Table 4, i.e., the $<S^2>$ value is 1.05 and 0.77 at the MP2 and B3LYP levels ($<S^2>$ is 0.75 for a pure doublet state), respectively. For the species **10** and **TS10/P1**, the $<S^2>$ values are 1.04 and 1.01 at the MP2 level, and 0.77 and 0.76 at the B3LYP level, respectively. The CC bond lengths within **10** and **TS10/P1** at the MP2 level are also significantly shorter than those at the B3LYP and QCISD levels. The QCISD method is known to have much less spin contamination. So, we do not decide to calculate the real QCISD $<S^2>$ values for these doublet species due to the expensive computational cost.

As shown in Table 4, the calculated B3LYP, MP2, and QCISD harmonic vibrational frequencies of H_2O and C_2H_2 are generally in good agreement with the experiments[42] with the maximum error being 8%. For the C_2H radical, the calculated C−C stretching and C−H bending frequencies deviate considerably from the experimental values[43] by about 14% and 12% (B3LYP), 34% and 125% (MP2), and 11% and 27% (QCISD), respectively. Surely, the MP2 method predicts the worst results for the C_2H radical. For **TS10/P1**, both B3LYP and MP2 predict much smaller imaginary frequencies with weaker intensities (in parentheses), i.e., 747i cm^{-1} (33 km/mol) and 1082i cm^{-1} (405 km/mol), respectively, than the QCISD value, 1638i cm^{-1} (1276 km/mol). The very large imaginary frequency with strong infrared intensity at the QCISD level is associated with the considerably shorter C(2)−H(4) bond (1.3976 Å) and H(4)−O(5) (1.0700 Å) than the corresponding B3LYP (1.4767 and 1.2174 Å) and MP2 (1.4746 and 1.1774 Å) values. Thus, the QCISD method predicts a much tighter transition state than B3LYP and MP2 do.

At the single-point CCSD(T)/6-311+G(3df,2p) level using the B3LYP/6-311G(d,p), MP2/6-311G(d,p), and QCISD/6-311G(d,p) geometries with the corresponding ZPVE correction, **10** almost has the same energy as **R**, i.e., at 0.7, −0.6, and −0.6 kcal/mol, respectively. The overall classical barrier height of this quasi-direct H-abstraction reaction via **TS10/P1** is 4.9, 5.1, and 3.7 kcal/mol at the single-point CCSD(T)/6-311+G(3df,2p) level with the B3LYP/6-311G(d,p), MP2/6-311G(d,p), and QCISD/6-311G(d,p) geometries, respectively. Such a H-abstraction process is exothermic. The B3LYP- and QCISD-based reaction heats are −15.1 and −16.0 kcal/mol, respectively, in close agreement with the value of −13.7 kcal/mol deduced from the experimental heat of formation (in kcal/mol at 298 K) of the species C_2H (135.0),[44] H_2O (−57.8),[45] C_2H_2 (54.2),[45] and OH (9.3).[45] The MP2-based reaction heat, 19.1 kcal/mol, deviates somewhat largely from the experimental value. This can surely be attributed to the rather short CC bond of the C_2H radical predicted by the MP2 method. The considerably larger stability of the weakly bound **10** relative to that of **R** predicted at the B3LYP level than at the other levels may be just a quantitative deficiency of the B3LYP method, since at the 6-311G(d,p) MP2 and QCISD levels, **10** still lies 3.9 and 3.4 kcal/mol below **R**, respectively. Zero-point energies play

important roles in determination of the relative energies of **10** and **TS10/P1**.

The QCISD-optimized structures and vibration frequencies for **TS10/P1** are surely expected to be superior to the B3LYP and MP2 results. By means of the calculated classical barrier height and vibrational frequencies of the critical structures **R**, **10**, **TS10/P1,** and **P1**, we can evaluate the rate constants of this quasi-direct H-abstraction within the conventional transition state theory (TST). The TST rate constants over a wide temperature range, 20−4500 K, are listed in Table 5. We can easily see that around the room temperature, the TST rate constants at the CCSD(T)/6-311+G(3df,2p)//QCISD/6-311G(d,p)+ZPVE level are very slow: $3.91 \cdot 10^{-16}$ (295 K) and $4.28 \cdot 10^{-16}$ cm^3 $molecule^{-1}$ s^{-1} (298 K).

Presumably, for such a quasi-direct H-abstraction reaction, the variational and tunneling effect may enhance the calculated rate constants especially at lower temperatures and thus should be considered. The minimum energy reaction path (MEP) is calculated by the IRC method. Subsequently, the force constant matrixes as well as the harmonic vibrational frequencies are calculated at some selected points along the MEP. Due to the rather expensive computational cost at the QCISD level, we decide just to make a crude estimate of the variational and tunneling effect from lower-level calculations. The energetic properties in Table 3 clearly show that without single-point energy correction, the B3LYP/6-311G(d,p) PES itself may lead us to the incorrect prediction that the C_2H+H_2O reaction proceeds without barrier to form **P1** due to the lower energy of **10** (−9.1 kcal/mol) and **TSP10/P1** (−5.5 kcal/mol) relative to **R**. Then, the B3LYP PES may be unsuitable for investigation of the dynamic properties of this quasi-direct H-abstraction process. On the other hand, the MP2/6-311G(d,p) PES itself can correctly describe the quasi-direct H-abstraction mechanism of the reaction with a considerable barrier, 3.5 kcal/mol. So, we utilize the MP2/6-311G(d,p) PES to calculate the TST, CVT, and CVT/SCT rate constants of this reaction as listed in Table 5 so as to estimate the variational and small curvature tunneling effect. We can easily find that (i) there is almost no variational effect over the whole temperature range, whereas the tunneling correction is very important below 298 K especially at very low temperatures; and (ii) there is a negative temperature dependence of rate constants below 80 K. The $k_{(CVT/SCT)}/k_{(TST)}$ ratio around the room temperature is 3.28 at 295 K and 3.21 at 298 K. We expect that similar variational and tunneling effects may exist at other levels within moderate temperatures. As a result, the final CVT/SCT rate constants of this quasi-direct H-abstraction process at the CCSD(T)/6-311+G(3df,2p)//QCISD/6-311G(d,p)+ZPVE level are still very slow: about $1.28 \cdot 10^{-15}$ (295 K) and $1.37 \cdot 10^{-15}$ cm^3 $molecule^{-1}$ s^{-1} (298 K). Also, at temperatures higher than 1000 K, the variational and tunneling effects already have negligible influence on the calculated rate constants, as indicated in the MP2/6-311G(d,p) results. The CCSD(T)/6-311+G(3df,2p)//QCISD/6-311G(d,p)+ZPVE TST rate constants only get considerable when $T > 1500$ K, i.e., $3.69 \cdot 10^{-12}$ and $1.07 \cdot 10^{-11}$ cm^3 $molecule^{-1}$ s^{-1} at 1500 and 2000 K, respectively. Therefore, the title reaction may be only significant at very high temperatures, such as those greater than 1500 K.

3.6. Comparison with Experiments and Other Reactions. To our knowledge, only one recent experiment by Van Look and Peeters[23] has been done on the C_2H+H_2O reaction. Their measured room-temperature rate constant $k_{(295K)}$ value is $(9.5 \pm 1.0) \cdot 10^{-12}$ cm^3 $molecule^{-1}$ s^{-1}. Notice that the experimental values of the analogous reactions of C_2H with H_2, CH_4, and C_2H_6 are $(4-5) \cdot 10^{-13}$,[18,19] $2.9 \cdot 10^{-12}$,[29] and $3.6 \cdot 10^{-11}$ cm^3 $molecule^{-1}$ s^{-1},[15] respectively. Given the corresponding H−X (X = OH, H, CH_3, C_2H_5) bond dissociation energies, i.e., 118, 103.3, 102.7, and 99 kcal/mol, it seems that the C_2H+H_2O reaction does not obey the empirical Polanyi−Evans type correlation between the $k_{(295K)}$ value and the H−X bond dissociation energy: i.e., the most exothermic reaction is the fastest. Van Look and Peeters[23] proposed that the C_2H+H_2O reaction might proceed via an association−elimination mechanism instead of a direct H-abstraction one for the C_2H reactions with H_2, CH_4, and C_2H_6.

Our investigation on the detailed C_2H_3O PES in proceeding sections clearly shows that the C_2H+H_2O radical reaction is still a simple quasi-direct H-abstraction process and the other dissociation or association−elimination processes are much less competitive. For the H-abstraction process at 295 K, at the CCSD(T)/6-311+G(3df,2p)//QCISD/6-311G(d,p)+ZPVE level, the calculated classical barrier height is 3.7 kcal/mol, which is larger than the theoretical values of 2.5 kcal/mol for the C_2H+H_2 reaction[36] and 2.4 kcal/mol for the C_2H+CH_4 reaction.[29] Notice that the barrier height for the C_2H+CH_4 reaction might be too high by about 0.7 or 1 kcal/mol as stated previously.[29] Furthermore, at the CCSD(T)/6-311+G(3df,2p)//QCISD/6-311G(d,p)+ZPVE level, the TST rate constant for the title reaction is $3.91 \cdot 10^{-16}$ cm^3 $molecule^{-1}$ s^{-1} and may increase to $1.28 \cdot 10^{-15}$ cm^3 $molecule^{-1}$ s^{-1} with inclusion of the rough estimate of the variational and tunneling effect. Surely, the theoretical rate constant is at least about 3 orders of magnitude smaller than the experimental value $(9.5 \pm 1.0) \cdot 10^{-12}$ cm^3 $molecule^{-1}$ s^{-1} determined by Van Look and Peeters. Over the whole temperature range, the estimated CVT/SCT rate constants of the C_2H+H_2O reaction at the CCSD(T)/6-311+G(3df,2p)//QCISD/6-311G(d,p)+ZPVE level is smaller than those of the C_2H+H_2 reaction at the G2//QCISD/6-311+G(d,p) level.[36] Within the temperature range 295−451 K at seven points, i.e., 295, 298, 332, 351, 385, 431, and 451 K, Van Look and Peeters obtained the Arrhenius expression as $k = (1.9 \pm 0.2) \cdot 10^{-11}\exp[(-200 \pm 30)/T(K)]$ cm^3 $molecule^{-1}$ s^{-1} with an almost zero upper-limit activation energy of 0.5 kcal/mol. Within the same temperature range, by means of our calculated CCSD(T)/6-311+G(3df,2p)/QCISD/6-311G(d,p)+ZPVE CVT/SCT rate constants, we can deduce an expression $2.10 \cdot 10^{-12}\exp[-2192/T(K)]$ cm^3 $molecule^{-1}$ s^{-1} with an activation energy of 4.4 kcal/mol. Clearly, both the theoretical Arrhenius frequency factor A and the activation energy E_a differ from the experimental values by a factor of about 10. At 295 K, even E_a is set to zero, and the theoretical k value is still smaller than the experimental one of $9.5 \cdot 10^{-12}$ cm^3 $molecule^{-1}$ s^{-1}.

It is very useful to assess the possible errors on the calculated barrier height and rate constants of this quasi-direct H-abstraction reaction. Future larger-scale and more complex computations [such as G3 single-point energies on QCISD geometries with larger basis sets than 6-311G(d,p)] may slightly reduce the present CCSD(T)/6-311+G(3df,2p)//QCISD/6-311G(d,p)+ZPVE barrier height of 3.7 kcal/mol and activation energy of 4.5 kcal/mol between 295 and 451 K. Yet the energetic reduction should not be too much, possibly around 1 kcal/mol. Another error may come from use of the small curvature tunneling correction incorporated in the *POLYRATE* program. As have been discussed by Hand et al.,[46] when the reaction path is acutely curved as in the H-transfer between two heavy fragments such as $HO+H_2O \rightarrow H_2O+OH$, the SCT method may provide an inadequate account for the tunneling. In this case, the large curvature tunneling correction may be more accurate,

which can only be used where an analytic representation of the potential-energy surface for a reaction is available. Unfortunately, the large curvature tunneling effect cannot be directly calculated by means of the ab initio PES alone. Then, it can only be inferred from similar H-transfer systems. For a typical H-transfer reaction X+HY→XH+Y, the angle β defined by the formula:

$$\cos^2\beta = \frac{m_X m_Y}{(m_X + m_H)(m_H + m_Y)} \quad (m \text{ is the effective mass})$$

can be used as an indicator of the acuteness of the reaction path curvature. Since the β value for the reaction HO+H_2O→H_2O+OH is 19°, Hand *et al.*[46] suggested that inclusion of the large curvature tunneling correction might produce a reduction of the activation barrier by 1.2 kcal/mol at 300 K. For the title C_2H+H_2O→C_2H_2+OH reaction with a β value of 20.5°, we assume a similar E_a reduction of about 1 kcal/mol due to inclusion of the large curvature tunneling correction.

Now with the possible error from the limited computational level and small curvature tunneling, a total reduction of about 2 kcal/mol for the activation energy may be introduced. Keeping in mind that an error of 2 kcal/mol can change a rate constant at 295 K by a factor of 30, the $k_{(295K)}$ value may then become $3.84 \cdot 10^{-14}$ cm^3 molecule^{-1} s^{-1}, which is still much lower than the experimental one of $2.9 \cdot 10^{-12}$ cm^3 molecule^{-1} s^{-1} by about 2 orders of magnitude.

Finally, we would like to discuss the possible errors introduced by the harmonic vibration approximation. Generally, internal rotation with low rotation barriers may have significantly higher partition functions than those of the corresponding fully harmonic vibrations. Moreover, their real ZPVE can be sizably lower than the harmonic ZPVE. Then, the frequency factor *A* may be increased. However, for the title quasi-direct H-abstraction reaction, the transition state **TS10/P1** has a very tight structure at the QCISD/6-311G(d,p) level, as shown in Figure 2. The three lowest frequencies, 110, 130 and 356 cm^{-1}, are still considerable. Moreover, due to the nearly isoenergetic nature of **10** relative to **R**, **10** may have negligible effect on calculation of the rate constants of the title reaction even though there are two vibration modes with very low values of 62 and 88 cm^{-1} for **10**. Thus, for the title reaction, influence of the nonharmonic vibration approximation on the calculated rate constants may be negligible.

Overall, our detailed mechanistic calculations at various levels definitively reveal that the C_2H+H_2O reaction is much slower than the C_2H+H_2 reaction. Both the barrier height and rate constants support that C_2H+H_2O is actually a normal quasi-direct H-abstraction reaction and is in accordance with the empirical Polanyi−Evans type correlation. The association−elimination mechanism proposed by Van Look and Peeters[23] involves much higher barriers and is thus almost negligible compared to the quasi-direct H-abstraction mechanism. We note that the rate coefficient data at 300 K for all of the other C_2H reactions measured with the same technique by this same group agree within 20% with the average of the existing experimental data.[23,24,29,30] We are not certain about the origin of such dramatic discrepancies between the theoretical and experimental rate constants. Yet, in view of the high quality of the present CCSD(T)/6-311+G(3df,2p)//QCISD/6-311G(d,p) calculations, we feel that it is very desirable to reinvestigate this reaction by measuring the rate constants and analyzing the products.

Due to the smaller rate constants of the C_2H+H_2O reaction obtained in our calculations, we can infer that the reaction of C_2H with H_2O may be of much less importance than that with H_2 and hydrocarbons in combustion modeling. It may also play a very minor role in the C_2H destruction process in dense interstellar space.

4. Conclusions

The mechanism of the C_2H+H_2O radical reaction is theoretically investigated at various levels. The most possible reaction pathway is a quasi-direct H-abstraction process with a barrier of 3.7 kcal/mol at the CCSD(T)/6-311+G(3df,2p)//QCISD/6-311G(d,p)+ZPVE level instead of an association−elimination process proposed by Van Look and Peeters. At 295 K, the estimated CVT/SCT rate constant of the C_2H+H_2O reaction is $1.28 \cdot 10^{-15}$ cm^3 molecule^{-1} s^{-1}, which is much smaller than the measured value of $(9.5 \pm 1.0) \cdot 10^{-12}$ cm^3 molecule^{-1} s^{-1} by Van Look and Peeters. It is shown that this H-abstraction reaction is much slower than the C_2H+H_2 and C_2H+CH_4 reactions. Therefore, the C_2H+H_2O radical reaction is just a normal direct H-abstraction one that satisfies the Polanyi−Evans type correction between the $k_{(295K)}$ value and the H−X bond dissociation energy (X = OH, H, CH_3, and C_2H_5). The surprisingly large discrepancies between our calculations and Van Look and Peeters's experimental results suggest that further laboratory investigations are very desirable for both kinetic and product analysis of this reaction.

Acknowledgment. We thank Professor Donald G. Truhlar for providing the *POLYRATE 8.0* program. This work is supported by the National Natural Science Foundation of China (No. 29892168, 20073014), Doctor Foundation of Educational Ministry, Foundation for University Key Teacher by the Ministry of Education, and Key Term of Science and Technology by the Ministry of Education of China. We are very thankful for the referee's invaluable comments on discussion of the possible errors of the calculated barrier height and rate constants.

References and Notes

(1) Shaub, W. M.; Bauer, S. H. *Combust. Flame* **1978**, *32*, 35.
(2) Kiefer, J. H.; Von Drasek, W. A. *Int. J. Chem. Kinet.* **1990**, *22*, 747.
(3) Kruse, T.; Roth, P. *J. Phys. Chem. A* **1997**, *101*, 2138.
(4) Tucker, K. D.; Kutner, M. L.; Thaddeus, P. *Astrophys. J.* **1974**, *193*, L11.
(5) Strobel, D. F. *Planet. Space Sci.* **1982**, *30*, 839.
(6) Lange, W.; Wagner, H. G. *Ber. Bunsen-Ges. Phys. Chem.* **1975**, *79*, 165.
(7) Laufer, A. H.; Bass, A. M. *J. Phys. Chem.* **1979**, *83*, 310.
(8) Laufer, A. H.; Bass, A. M. *J. Phys. Chem.* **1981**, *85*, 3823.
(9) Okabe, H. *J. Phys. Chem.* **1982**, *78*, 1312.
(10) Laufer, A. H.; Lechleider, R. *J. Phys. Chem.* **1984**, *88*, 66.
(11) Renlund, A. M.; Shokoohi, F.; Reisler, H.; Wittig, C. *Chem. Phys. Lett.* **1981**, *84*, 293.
(12) Renlund, A. M.; Shokoohi; F.; Reisler, H. C. *J. Phys. Chem.* **1982**, *86*, 4165.
(13) Stephens, J. W.; Hall, J. L.; Solka, H.; Yan, W.-B.; Curl, R. F.; Glass, G. P. *J. Phys. Chem.* **1987**, *91*, 5740.
(14) Lander, D. R.; Unfried, K. G.; Stephen, J. W.; Glass, G. P.; Curl, R. F. *J. Phys. Chem.* **1989**, *93*, 4109.
(15) Lander, D. R.; Unfried, K. G.; Glass, G. P.; Curl, R. F. *J. Phys. Chem.* **1990**, *94*, 7759.
(16) Shin, K. S.; Michael, J. V. *J. Phys. Chem.* **1991**, *95*, 5864.
(17) Koshi, M.; Nishida, N.; Matsui, H. *J. Phys. Chem.* **1992**, *96*, 5875.
(18) Koshi, M.; Fukuda, K.; Matsui, H. *J. Phys. Chem.* **1992**, *96*, 9839.
(19) Farhat, S. K.; Morter, C. L.; Glass, G. P. *J. Phys. Chem.* **1993**, *97*, 12789.
(20) Opansky, B. J.; Seakins, P. W.; Pedersen, J. O. P.; Leone, S. R. *J. Phys. Chem.* **1993**, *97*, 8583.
(21) Opansky, B. J.; Leone, S. R. *J. Phys. Chem.* **1996**, *100*, 4888.
(22) Opansky, B. J.; Leone, S. R. *J. Phys. Chem.* **1996**, *100*, 19904.
(23) Van Look, H.; Peeters. J. *J. Phys. Chem.* **1995**, *99*, 16284.
(24) Peeters, J.; Van Look, H.; Ceursters, B. *J. Phys. Chem.* **1996**, *100*, 15124.

(25) Hoobler, R. J.; Opansky, B. J.; Leone, S. R. *J. Phys. Chem. A.* **1997**, *101*, 1338.
(26) Kruse, T.; Roth, P. *J. Phys. Chem.* **1997**, *101*, 2138.
(27) Chastaing, D.; James, P. I.; Sims, I. R.; Smith, I. W. M. *Faraday Discuss.* **1998**, *109*, 165.
(28) Su, H.; Yang, J.; Ding, Y.; Feng, W.; Kong, F. *Chem. Phys. Lett.* **2000**, *325*, 73.
(29) Ceursters, B.; Nguyen, H. M. T.; Peeters, J.; Nguyen, M. T. *Chem. Phys. Lett.* **2000**, *328*, 412.
(30) Ceursters, B.; Nguyen, H. M. T.; Peeters, J.; Nguyen, M. T. *Chem. Phys.* **2000**, *262*, 243.
(31) Harding, L. B.; Schatz, G. C.; Chiles, R. A. *J. Chem. Phys.* **1982**, *76*, 5172.
(32) Herbst, E. *Chem. Phys. Lett.* **1994**, *222*, 297.
(33) Wang, D. S.; Bowman, J. M. *J. Chem. Phys.* **1994**, *101*, 8646.
(34) Sumathi, R.; Peeters, J.; Nguyen, M. T. *Chem. Phys. Lett.* **1998**, *287*, 109.
(35) Sengupta, D.; Peeters, J.; Nguyen, M. T. *Chem. Phys. Lett.* **1998**, *91*, 283.
(36) Zhang, X.; Ding, Y. H.; Li, Z. S.; Huang, X. R.; Sun, C. C. *J. Phys. Chem. A* **2000**, *104*, 8375.
(37) Frisch, M. J.; Trucks, G. W.; Schlegel, H. B.; Scuseria, G. E.; Robb, M. A.; Cheeseman, J. R.; Zakrzewski, V. G.; Montgomery, J. A., Jr.; Stratmann, R. E.; Burant, J. C.; Dapprich, S.; Millam, J. M.; Daniels, A. D.; Kudin, K. N.; Strain, M. C.; Farkas, O.; Tomasi, J.; Barone, V.; Cossi, M.; Cammi, R.; Mennucci, B.; Pomelli, C.; Adamo, C.; Clifford, S.; Ochterski, J.; Petersson, G. A.; Ayala, P. Y.; Cui, Q.; Morokuma, K.; Malick, D. K.; Rabuck, A. D.; Raghavachari, K.; Foresman, J. B.; Cioslowski, J.; Ortiz, J. V.; Stefanov, B. B.; Liu, G.; Liashenko, A.; Piskorz, P.; Komaromi, I.; Gomperts, R.; Martin, R. L.; Fox, D. J.; Keith, T.; Al-Laham, M. A.; Peng, C. Y.; Nanayakkara, A.; Gonzalez, C.; Challacombe, M.; Gill, P. M. W.; Johnson, B. G.; Chen, W.; Wong, M. W.; Andres, J. L.; Head-Gordon, M.; Replogle, E. S.; Pople, J. A. *Gaussian 98*; Gaussian, Inc.: Pittsburgh, PA, 1998.
(38) Chuang, Y.-Y.; Corchado, J. C.; Fast, P. L.; Villà, J.; Hu, W.-P.; Liu, Y.-P.; Lynch, G. C.; Nguyen, K. A.; Jackels, C. F.; Gu, M. Z.; Rossi, I.; Coitiño, E. L.; Clayton, S.; Melissas, V. S. *POLYRATE*, ver. 8.0, University of Minnesota, 1998.
(39) Hunziker, H. E.; Kneppe, H.; Wendt. H. R. *J. Photochem.* **1981**, *12*, 377.
(40) Osborn, D. L.; Choi, H.; Mordaunt, D. H.; Bise, R. T.; Neumark, D. M.; Rohlfing, C. M. *J. Chem. Phys.* **1997**, *106*, 3049.
(41) Bogey, M.; Demuynck, C.; Destombes, J. L. *Mol. Phys.* **1989**, *66*, 955.
(42) Lide, D. R. In *CRC Handbook of Chemistry and Physics*, 79th ed.; CRC Press: New York, 1998.
(43) Temsamani, M. A.; Herman, M. *J. Chem. Phys.* **1995**, *102* (16), 6371.
(44) Back, W. H.; Mackie, J. C. *J. Chem. Soc., Faraday Trans.* **1975**, *71*, 1363.
(45) Chase, M. W., Jr. *NIST-JANAF Thermochemical Tables*, 4th Edition; *J. Phys. Chem. Ref. Data, Monograph 9*, **1998**, 1−1951.
(46) Hand, M. R.; Rodriquez, C. F.; Williams, I. H.; Balint-Kurti, G. G. *J. Phys. Chem.* **1998**, *102*, 5958.